

Research Article: New Research | Disorders of the Nervous System

## The Ventral Pallidum Innervates a Distinct Subset of Midbrain Dopamine Neurons

<https://doi.org/10.1523/ENEURO.0222-25.2025>

Received: 7 June 2025

Revised: 25 June 2025

Accepted: 12 September 2025

Copyright © 2025 Yang et al.

This is an open-access article distributed under the terms of the [Creative Commons Attribution 4.0 International license](#), which permits unrestricted use, distribution and reproduction in any medium provided that the original work is properly attributed.

---

*This Early Release article has been peer reviewed and accepted, but has not been through the composition and copyediting processes. The final version may differ slightly in style or formatting and will contain links to any extended data.*

**Alerts:** Sign up at [www.eneuro.org/alerts](http://www.eneuro.org/alerts) to receive customized email alerts when the fully formatted version of this article is published.

**TITLE:** The Ventral Pallidum Innervates a Distinct Subset of Midbrain Dopamine Neurons

**ABBV TITLE:** Ventral Pallidum Targets Subset of Dopamine Neurons

**AUTHORS:** Olivia J. Yang<sup>1</sup> B.S., Hannah B. Elam<sup>1</sup> PhD., Kayla Lilly<sup>1</sup> B.S., Alexandra M. McCoy<sup>1</sup> PhD., Valeriia Klepikova<sup>1</sup>, Stephanie M. Perez<sup>1</sup> PhD., and Daniel J. Lodge<sup>1,2</sup> Ph.D.

**AFFILIATIONS:**

1 Department of Pharmacology and Center for Biomedical Neuroscience, University of Texas Health Science Center, San Antonio, TX, 78229, USA

2 South Texas Veterans Health Care System, Audie L. Murphy Division, San Antonio, USA

**Author Contributions:** O.J.Y. made contributions to the design of the work, acquisition, analysis and interpretation of the data, as well as drafting the manuscript. H.B.E., K.L., A.M.M., and V.K. made contributions to acquisition and analysis of the data. S.M.P and D.J.L both contributed to the concept and design of the study, interpretation of the data, revising and editing manuscript content, as well as providing final approval of the document.

**CORRESPONDING AUTHOR:**

Olivia Yang

University of Texas Health Science Center

Department of Pharmacology

7703 Floyd Curl Drive

San Antonio, TX, 78229

Email: yango@livemail.uthscsa.edu

**Number of Figures:** 3

**Number of words for Abstract:** 250

**Number of Tables:** 1

**Number of words for Significance Statement:** 120

**Number of Multimedia:** 0

**Number of words for Introduction:** 690

**Number of words for Discussion:** 2501

**Acknowledgements:** We would like to thank Dr. David Morilak for thoughtful discussions on the topic that inspired the conceptualization of this work.

**Funding:** This work was supported by Merit Awards #BX004693 and #BX004646 from the United States Department of Veterans Affairs, Biomedical Laboratory Research and Development Service (to D.J.L.), the National Institutes of Health R01-AG076030, T32-NS082145 (to O.J.Y., H.B.E., K.L., and A.M.M.), and F31-MH127890-01A1 to H.B.E.

**Animal Statement:** All experiments were performed in accordance with guidelines outlined in the USPH Guide for the Care and Use of Laboratory animals and were approved by the Institutional Animal Care and the Use Committees of UT Health San Antonio and the US Department of Veterans Affairs

## 1 **ABSTRACT**

2 Aberrant dopamine transmission is a hallmark of several psychiatric disorders. Dopamine neurons in the ventral  
3 tegmental area (VTA) display distinct activity states that are regulated by discrete afferent inputs. For example,  
4 burst firing requires excitatory input from the mesopontine-tegmentum, while dopamine neuron population  
5 activity, defined as the number of spontaneously active dopamine neurons, is thought to be dependent on  
6 inhibitory drive from the ventral pallidum (VP). Rodent models used to study psychiatric disorders, such as  
7 psychosis, consistently exhibit elevated dopamine neuron population activity, due to decreased tonic inhibition  
8 from the VP. However, it remains unclear whether the VP can modulate all dopamine neurons, or if only a specific  
9 subset of VTA dopamine neurons receive innervation from the VP to be recruited as required. This knowledge  
10 is critical for understanding dopamine regulation in normal and pathological conditions. Here, we used in vivo  
11 electrophysiology in male and female rats to record VTA dopamine neurons inhibited by electrical stimulation of  
12 the VP. Specifically, VP stimulation inhibited ~22% of spontaneously active dopamine neurons; however,  
13 activation of the ventral hippocampus, a modulator of VTA population activity, increased the proportion to ~48%.  
14 This increase suggests that VP selectively modulates a subset of dopamine neurons that can be recruited by  
15 afferent activation. Anterograde monosynaptic tracing revealed that approximately half of the VTA dopamine  
16 neurons receive input from the VP. Taken together, we demonstrate that a subset of VTA dopamine neurons  
17 receive monosynaptic input from the VP, which provides valuable information regarding the regulation of VTA  
18 neuron activity.

## 19 **SIGNIFICANCE STATEMENT**

20 Dysregulated dopamine signaling has been linked to many psychiatric disorders. Therefore, understanding how  
21 dopamine neuron activity is regulated is essential for identifying mechanisms contributing to normal and  
22 pathologic states. Dopamine neuron population activity refers to a dynamic collection of neurons that can be  
23 recruited to assign salience to stimuli. This activity state is known to be regulated by afferent inputs to the ventral  
24 pallidum, which provides a tonic inhibition to dopamine neurons. This study demonstrates that the VP provides  
25 flexible, targeted control of dopamine signaling. These findings improve our understanding of how dopamine  
26 activity is regulated and may help guide future treatments for psychiatric disorders involving dopamine  
27 dysfunction.

## 28 INTRODUCTION

29 The dopamine system plays a central role in numerous processes, including motivation, reward learning,  
30 salience attribution, decision-making, and cognitive flexibility(Baik & Baik, 2020; Klein et al., 2019). When this  
31 system becomes dysregulated, it can lead to pathological states characterized by altered perception, affect, and  
32 motivation(Baik & Baik, 2020; Finlay & Zigmond, 1997; Klein et al., 2019). Indeed, aberrant dopamine signaling  
33 has been implicated in a wide range of psychiatric disorders, including schizophrenia, psychosis, depression,  
34 bipolar disorder, and substance use disorders(Ashok et al., 2017; Belujon & Grace, 2014; Compean & Hamner,  
35 2019; Egerton et al., 2013; Grace, 1995, 2000; Howes et al., 2009; Volkow et al., 2004). In the case of  
36 schizophrenia and psychosis, patients exhibit a hyperdopaminergic state, particularly within subcortical regions  
37 such as the striatum(Abi-Dargham et al., 1998; Howes et al., 2012; Howes et al., 2009; Laruelle & Abi-Dargham,  
38 1999). This increase in dopamine system function is thought to underlie the phenomenon of aberrant salience,  
39 where neutral or irrelevant stimuli are assigned inappropriate significance, contributing to the development of  
40 delusions and hallucinations(Kapur, 2003; Palaniyappan & Liddle, 2012). Thus, understanding the mechanisms  
41 that regulate dopamine system output is critical for elucidating the neural basis of psychiatric illnesses and  
42 identifying targets for therapeutic intervention.

43 The cell bodies of mesolimbic dopamine neurons reside in the ventral tegmental area (VTA), and these neurons  
44 can exist in two distinct activity states: active (single spike and burst firing) and inactive (hyperpolarized)(Grace  
45 & Bunney, 1984a, 1984b). Advances in electrophysiological techniques have demonstrated that under normal  
46 conditions, only a certain number of dopamine neurons in the VTA are spontaneously active, while the rest are  
47 kept in an inactive, hyperpolarized state(Grace & Bunney, 1985). This observation led to the establishment of a  
48 third activity state, population activity, used to describe the number of spontaneously firing dopamine neurons.  
49 These “silent” dopamine neurons can be recruited to assign salience to an event or chronically altered under  
50 certain pathological states(Lodge & Grace, 2006). For example, rodent models used to study psychosis  
51 consistently demonstrated dramatic increases in dopamine neuron population activity(Aguilar, 2014; Elam et al.,  
52 2021; Lodge & Grace, 2007; Lodge & Grace, 2009), while models used to study stress-induced depression-like  
53 behaviors report pathological decreases in activity(Chang & Grace, 2013a, 2013b). Moreover, it has been

54 previously shown that increased dopamine neuron population activity, leads to increased dopamine synthesis  
55 capacity that is observed in rodent models and patients with psychosis (Howes et al., 2012; Howes et al., 2009;  
56 Perez et al., 2022). This subset of dopamine neurons is essential for regulating salience and the aberrant  
57 dopaminergic signaling seen in psychiatric disorders such as psychosis and depression. However, the  
58 mechanisms involved in this regulation are not yet fully understood. The regulation of dopamine neuron  
59 population activity is a complex process involving multiple brain regions (Figure 1). Previous research showed  
60 that the ventral pallidum (VP) exerts a significant inhibitory influence on dopamine neurons through GABA-ergic  
61 projections to the VTA (Floresco et al., 2001; Floresco et al., 2003; Grace & Bunney, 1985; Mahler et al., 2014;  
62 Watabe-Uchida et al., 2012). Glutamatergic inputs from the ventral hippocampus (vHipp) and paraventricular  
63 nucleus of the thalamus converge in the nucleus accumbens (NAc) to modulate projections to the VP (Perez &  
64 Lodge, 2018). Disruptions in the regulation of this circuit lead to the disinhibition of dopamine neurons through  
65 increased inhibitory drive from the NAc to the VP (Aguilar, 2014). Interestingly, rodent models used to study  
66 schizophrenia display increased dopamine neuron population activity due to heightened hippocampal activity,  
67 while rodents exposed to acute stressors, such as foot shocks, exhibit a similar phenotype, though this is  
68 mediated by hyperactivity in the thalamus (Elam et al., 2025; Floresco et al., 2001; Floresco et al., 2003; Lodge  
69 & Grace, 2007, 2008b; Perez & Lodge, 2018). Conversely, decreases in dopamine neuron population activity  
70 are observed following chronic mild stress, and are associated with a more depressive-like phenotype via  
71 increased excitatory transmission from the basolateral amygdala to VP (Chang & Grace, 2013a, 2013b). Although  
72 we have gained some insights, we still do not fully understand how the projections from the VP to VTA influence  
73 dopamine neuron activity. One possibility is that the VP forms synaptic connections with the majority of VTA  
74 dopamine neurons, but selectively inhibits them based on specific inputs. Alternatively, the VP may target only  
75 a subpopulation of dopamine neurons, allowing for the recruitment of a distinct pool of dopamine neurons.  
76 Understanding these mechanisms is essential for elucidating the pathophysiology of various psychiatric  
77 disorders and for developing targeted therapeutic interventions.

78 In this study, we aim to address these knowledge gaps by investigating the role of VP projections in controlling  
79 VTA dopamine neuron population activity. We performed in vivo electrophysiology to record from dopamine  
80 neurons while simultaneously stimulating the VP to determine the percent of spontaneously active dopamine

neurons that can be inhibited by VP. Furthermore, we utilized a monosynaptic tracer to map the projections from VP to VTA, providing an anatomical framework for understanding these interactions. Our findings shed new light on the neural circuits involved in dopaminergic regulation that are disrupted under conditions such as psychosis.

## **MATERIALS AND METHODS**

All experiments were performed in accordance with guidelines outlined in the USPH Guide for the Care and Use of Laboratory animals and were approved by the Institutional Animal Care and the Use Committees of UT Health San Antonio and the US Department of Veterans Affairs

### *Animals*

Studies were performed on adult male and female Sprague Dawley (SD) rats (250-600 g; Envigo; Indianapolis, IN, USA) that were group-housed (2-3 per cage). All rats were housed in a temperature-controlled environment, maintained on a 12-hour light/12-hour dark cycle, and provided with ad libitum access to food and water.

### *Dopamine neuron electrophysiology*

Rats were anesthetized with 8% chloral hydrate (400 mg/kg *i.p.*; C8383, Sigma-Aldrich) and placed in a stereotaxic apparatus for the duration of the experiments. Supplemental anesthesia was administered as required to maintain suppression of the limb compression withdrawal reflex. A thermostatically controlled heating pad (PhysioSuite, Kent Scientific Corporation, Torrington, CT, USA) was used to maintain a core body temperature of 37 °C. Extracellular glass microelectrodes (impedance ~6-10 MΩ) were lowered into the VTA (AP -5.3 mm, ML ± 0.6 mm from bregma, and DV -6.5-9.0 mm ventral of the brain surface) using a hydraulic micro-positioner (Model 640; Kopf Instruments; Tujunga, CA, USA). Spontaneously active dopamine neurons were identified using previously established electrophysiological criteria (action potential >2ms, firing rate between 0.5-15 Hz) (Grace & Bunney, 1983b; Ungless & Grace, 2012) and open filter settings (low-frequency cutoff: 30 Hz; high-frequency cutoff: 30 kHz). The electrodes were lowered to make 6-12 vertical passes through the VTA in a predetermined pattern separated by 200 μm, thereby allowing various regions of the VTA to be sampled. Three parameters of dopamine activity were measured and analyzed: the number of dopamine neurons firing spontaneously (population activity)(Grace & Bunney, 1983a), basal firing rate, and proportion of

106 action potentials occurring in bursts (defined as the incidence of spikes with <80 ms between them; termination  
107 of the burst is defined as >160 ms between spikes)(Grace & Bunney, 1983a). Analysis of dopamine neuron  
108 activity was performed using commercially available computer software (LabChart version 8; ADInstruments,  
109 Colorado Springs, CO, USA).

110 To examine VP regulation of the VTA, a bipolar, concentric-stimulating electrode (World Precision Instruments,  
111 Sarasota, FL, USA) was lowered into the VP (AP -0.0 mm, ML  $\pm$  2.3 mm from bregma, and DV -9.0 mm ventral  
112 of the brain surface). Once a stable spontaneously active dopamine neuron was identified, a baseline of 1 minute  
113 was recorded followed by 2 minutes of VP stimulation using single-current pulses (0.25 ms; 1.0 mA; 0.5 Hz;  
114 Figure 2J). To determine whether a dopamine neuron was excited or inhibited by the electrical stimulation,  
115 peristimulus time histograms (Figure 2I) were generated and criteria of  $\geq 2$  consecutive bins (50 ms) that were  
116 greater (for excited neurons) or lower (for inhibited neurons) than 2 standard deviations from the average  
117 baseline(Lodge, 2011). For neurons where 2 standard deviations below the baseline was negative, a criteria of  
118  $\geq 2$  consecutive bins of 0 was used to define inhibition.

119 For intracranial drug administration of NMDA (0.75  $\mu$ L of 1.5mg/ml; M3262, Sigma-Aldrich) or vehicle [Dulbecco's  
120 PBS (dPBS); 0.75  $\mu$ L; 59331C, Sigma-Aldrich), a 26-gauge canula (Plastics One; Roanoke County, VA, USA)  
121 was lowered into the vHipp (AP -5.3 mm, ML  $\pm$  5.0 mm from bregma, DV -7.0 mm ventral of the brain surface).  
122 An internal canula (Plastics One), extending 1 mm past the end of the guide canula was used to deliver a one-  
123 time injection administered at a rate of 0.5 $\mu$ L/min ~10 min prior to electrophysiology recordings.

#### 124 *Trans-synaptic viral tracing*

125 Rats were anesthetized with Fluriso (2-5% isoflurane, USP, with oxygen flow at 1 L/min) and placed in a  
126 stereotaxic apparatus using blunt atraumatic ear bars. A core body temperature of 37°C was maintained. Rats  
127 had a cannula implanted bilaterally in the VP (AP -0.0 mm, ML  $\pm$  2.3 mm from bregma, and DV -8.0 mm ventral  
128 of the brain surface) and the herpes helper virus AAV2-hSYN-TK was injected(Zeng et al., 2017) (0.5  $\mu$ L/2 x 10<sup>11</sup>  
129 GC/mL; VectorBuilder) through an injector that extended 1 mm past the cannula tip. Three weeks following the  
130 initial injection, the replication-incompetent monosynaptic anterograde herpes simplex virus type 1 strain  
131 (H129- $\Delta$ TK-tdTomato) was bilaterally injected in the VP(Zeng et al., 2017) (UCI; 0.5  $\mu$ L/2.75 x 10<sup>5</sup> PFU). This

132 virus has a deleted thymidine kinase (TK) gene stopping it from replicating or spreading in neurons. When  
133 complementarily expressed with TK from the helper virus, H129- $\Delta$ TK-tdT can map the direct monosynaptic  
134 projections of the transfected neurons(Zeng et al., 2017).

### 135 *Immunohistochemistry*

136 Ten days after the H129- $\Delta$ TK-tdTomato administration, rats were deeply anesthetized with 8% chloral hydrate  
137 (400 mg/kg *i.p.*) and transcardially perfused with saline followed by 4% formaldehyde. Brains were removed,  
138 post-fixed overnight, and cryoprotected (10% w/v sucrose in PBS) until saturated. Brains were sectioned  
139 coronally (50  $\mu$ m) using a cryostat (Leica; Buffalo Grove, IL, USA), and sections containing the VTA were stored  
140 in PBS. Sections were washed three times (10 minutes) in PBS then blocked (2% normal goat serum, 0.3%  
141 Triton-X 100) for 30 minutes at room temperature. Primary antibodies [rabbit anti-tyrosine hydroxylase 1:1000  
142 (ab112, Abcam); chicken anti-red fluorescent protein 1:1000 (409 006, Synaptic Systems)] were applied (in PBS  
143 containing 1% normal goat serum, 0.3% Triton-X 100) overnight at 4°C. Secondary antibodies [AlexaFluor® 488  
144 goat anti-rabbit 1:1000 (A-11008, ThermoFisher); AlexaFluor® 594 goat anti-chicken 1:1000 (A-11042,  
145 ThermoFisher)] for 1 hour at room temperature. Slices were then mounted and cover slipped with ProLong gold  
146 anti-fade reagent (P36930, ThermoFisher).

### 147 *Monosynaptic Neuron Quantification*

148 Immunostained sections (2 – 5 per animal) were imaged using an inverted fluorescent microscope (Axio  
149 Observer Z1, Zeiss) with 63X oil objective to capture high resolution images of VTA. Cell quantification was  
150 performed manually using ImageJ software with the Colocalization Object Counter(Lunde et al., 2020–11–04).  
151 Dopamine neurons were quantified by counting TH+ cells in the green 488 channel, while cells receiving direct  
152 monosynaptic input from the VP were quantified by counting tdTomato+ cells in the red 594 channel. To  
153 determine the spatial distribution of TH+ and tdTomato+ cells, sections were grouped and analyzed according  
154 to stereotaxic coordinates. For each slice, the VTA was divided into three sections from medial to lateral: ([0.00  
155 to 0.60], [0.60 to 1.3], [1.3 to 2.0] mm from bregma). Brain sections were categorized into 4 groups from anterior  
156 to posterior ([-4.7 to -5.0], [-5.0 to -5.4], [-5.4 to -5.8], and [-5.8 to -6.1] mm from bregma).

### 157 *Histological Verification of Electrode Locations*

Rats used for electrophysiology were rapidly decapitated following recordings, and brains were dissected out, post-fixed, cryoprotected, and sectioned coronally (25  $\mu$ m). Sections containing electrode or cannula tracks were mounted onto gelatin-chrome-coated slides, stained with neutral red (0.1%) and thionin acetate (0.01%), and cover slipped with DPX Mountant (06522, Sigma-Aldrich) for histological confirmation of the recording electrode (Figure 2G), stimulating electrode (Figure 2G), or cannula (vHipp: Figure 2H, VP: Figure 3B) with reference to a stereotaxic atlas (Paxinos, 1998).

### *Statistical Analysis*

Electrophysiological analysis of dopamine neuron activity was performed using commercially available computer software (Lab Chart version 8; ADInstruments Ltd.; Chalgrove, Oxfordshire, UK). Data are represented as the mean  $\pm$  SEM with n values representing the number of rats per experimental group, unless otherwise stated. Proportions of dopamine neurons inhibited and unchanged by VP stimulation were determined by Chi-Square, while other metrics of dopamine neuron activity were analyzed by t-test or two-way ANOVA (Vehicle/NMDA x Stimulation on/off) and the Holm-Sidak post-hoc test was used when significant interactions were determined (Table 1). When assumptions of normality were violated, Mann-Whitney or Aligned Rank Transform (ART) ANOVA were used. Statistics were calculated using Prism software (Version 10; GraphPad Software Inc., San Diego CA, USA) or R-4.5.0 with significance determined at  $p < 0.05$ , and graphed with Prism software.

## **RESULTS**

### *Proportion of dopamine neurons inhibited by VP stimulation increases following vHipp activation*

To determine the proportion of VTA dopamine neurons inhibited by VP stimulation under normal conditions and during hippocampal activation, we used in vivo extracellular electrophysiology with electrical stimulation of the VP (Figure 2). In vehicle-treated animals, 21.9% of dopamine neurons were inhibited by VP stimulation, 10.5% were excited, and 67.6% exhibited no change ( $n = 105$  dopamine neurons from 11 rats, Figure 2A). We next wanted to determine if activation of the vHipp, which indirectly attenuates inhibition from the VP to the VTA, would change the proportion of dopamine neurons responding to VP stimulation. Interestingly, following NMDA activation of vHipp, the percentage of dopamine neurons inhibited by VP stimulation increased to 49.5% and the

184 corresponding dopamine neurons that did not respond to stimulation decreased to 39.8% ( $n= 103$  dopamine  
 185 neurons, 9 rats). The percentage of excited neurons remained the same at 10.7%. There was a significant  
 186 difference in the proportion of inhibited and unchanged neurons between vehicle and NMDA-treated animals  
 187 (Chi-Square = 18.61;  $p < 0.0001$ ; Figure 2A).

188 Consistent with previous studies, rats receiving vehicle in vHipp exhibited  $1.11 \pm 0.07$  cells per track ( $n= 11$  rats),  
 189 and this was significantly increased to  $1.70 \pm 0.12$  cells per track ( $n= 9$  rats) following NMDA administration (t  
 190 test;  $t= 4.38$ ;  $p= 0.0004$ ; Figure 2B). Furthermore, vHipp activation did not alter burst firing ( $n= 99$  neurons,  $29.6$   
 191  $\pm 2.7\%$  burst firing) compared to vehicle ( $n= 105$  neurons,  $28.3 \pm 2.4\%$  burst firing; Mann Whitney,  $U= 5131$ ,  $p=$   
 192  $0.875$ , Figure 2C). vHipp NMDA also did not alter baseline firing rate ( $n= 99$  neurons,  $3.47 \pm 0.19$  Hz) compared  
 193 to vehicle ( $n= 105$  neurons,  $3.56 \pm 0.19$  Hz; t-test,  $t= 0.361$ ,  $p= 0.719$ ). Repeated VP stimulation had no sustained  
 194 effect on average firing rate in vehicle ( $n= 105$  neurons,  $3.19 \pm 0.19$  Hz) or NMDA ( $n= 99$  neurons,  $3.43 \pm 0.2$   
 195 Hz; ART ANOVA,  $F_{(1,407)Stimulation}=1.287$ ,  $p= 0.257$ ;  $F_{(1,407)Treatment}= 0.282$ ,  $p= 0.596$ ; Figure 2D) treated animals.  
 196 Additionally, we examined whether firing frequency or burst firing predict the response to VP stimulation.  
 197 Interestingly we found no effect of stimulation response on firing frequency (No Change:  $n= 108$  neurons,  $3.37$   
 198  $\pm 0.19$  Hz; Excited:  $n= 22$  neurons,  $3.23 \pm 0.46$  Hz; Inhibited:  $n= 74$  neurons,  $3.82 \pm 0.21$  Hz; Kruskal-Wallis,  
 199  $KW= 4.622$ ,  $p= 0.0922$ ; Figure 2E) or burst firing (No Change:  $25.40 \pm 2.34\%$ ; Excited:  $38.47 \pm 5.62\%$ ; Inhibited:  
 200  $31.5 \pm 3.14\%$ ; Kruskal-Wallis,  $KW= 5.691$ ,  $p= 0.058$ ; Figure 2F). Taken together, these data support the  
 201 hypothesis that the VP regulates tonic inhibition of VTA dopamine neurons. Given that the proportion of  
 202 dopamine neurons inhibited by VP is increased under NMDA activation of vHipp, it is likely that the VP innervates  
 203 a subset of dopamine neurons in the VTA, rather than regulating a more sizable proportion of the population of  
 204 neurons.

### 205 *Monosynaptic Projections from the VP innervate ~50% of VTA dopamine neurons*

206 To validate these findings anatomically, we used the anterograde monosynaptic Herpes virus to label projections  
 207 from the VP to VTA (Figure 3A). We used a TH-antibody to label dopamine neurons in the VTA (Figure 3C) and  
 208 counted the proportion of dopamine neurons receiving monosynaptic inputs from the VP. We found that  $50.4 \pm$   
 209  $6.7\%$  of TH+ cells were tdTomato+, indicating that VP innervates about half of dopamine neurons in VTA (Figure

3D-E). Interestingly,  $47.9 \pm 5.4\%$  of tdTomato+ cells were TH+, indicating that VP also innervates a substantial number of non-dopaminergic cells in VTA. To determine if dopamine neurons innervated by the VP were localized to specific regions of VTA, we analyzed colocalized cells based on anatomical position. The average number of colocalized cells per animal was  $35.5 \pm 5.8$  for the most medial portion of VTA,  $40.5 \pm 6.5$  in the center, and  $42.2 \pm 8.8$  for the most lateral portion of VTA. One-way ANOVA revealed no significant differences in colocalized cells between VP subregions medial to lateral ( $F_{(2,15)} = 0.2423$ ,  $p = 0.7879$ , Figure 3F). Similarly, no significant differences were observed between subregions anterior to posterior ([anterior  $\rightarrow$  posterior]  $103.0 \pm 24.7$ ,  $164.2 \pm 19.2$ ,  $166.5 \pm 29.0$ ,  $74.3 \pm 17.4$ ;  $F_{(3,11)} = 2.999$ ,  $p = 0.0769$ , Figure 3G). These data indicate that VP heterogeneously innervates a subset of dopamine neurons in the VTA.

## DISCUSSION

Aberrant dopamine system function contributes to numerous psychiatric disorders including psychosis, which is believed to be driven by an increase in the number of spontaneously active dopamine neurons in the VTA (Abi-Dargham, 2004; Howes et al., 2009; Lodge & Grace, 2008b; Perez et al., 2022). This activity state, termed population activity, has been extensively examined and known to be regulated by multisynaptic circuits involving many brain regions, including the PVT, BLA, vHipp, and NAc, ultimately converging on VP inputs to the VTA (Chang & Grace, 2013a, 2013b; Lodge & Grace, 2008b; Perez & Lodge, 2018). In vivo intracellular recordings from VTA dopamine neurons have demonstrated that a proportion of these neurons are bombarded by miniature inhibitory postsynaptic potentials, likely from the VP, which results in an absence of spontaneous activity (Grace & Bunney, 1985). This activity state seems essential for the proper functioning of the dopamine system, but it remains unclear whether a majority of VTA dopamine neurons are innervated by the VP. Further, it is not clear if this connection orchestrates the activation of specific neurons or if only a particular subset of neurons are inhibited by the VP resulting in a silent 'pool' of neurons available to be recruited. Here, we demonstrate that the second theory appears correct: the VP only innervates a subset of VTA dopamine neurons that are distinguishable based on their response to VP stimulation under our recording conditions. This indicates that changes in the overall activity of dopamine neurons are influenced by the activity of a distinct collection of dopamine neurons that are selectively innervated by the VP.

236 Studies on the innervation from VP to the VTA consistently indicate that VP GABA neurons project to VTA  
237 dopamine neurons(Faget et al., 2016; Li et al., 2020; Palmer et al., 2024). Retrograde tracing studies indicate  
238 that projections from the VP to VTA are largely inhibitory, as over 90% of VP neurons projecting to the VTA  
239 express the GABA synthesizing enzyme glutamic acid decarboxylase(Palmer et al., 2024). However, previous  
240 studies have not investigated the specific VTA neuron population receiving input from the VP. In our studies, we  
241 employ extracellular electrophysiology to record from individual dopamine neurons in vivo. We found that at  
242 baseline, approximately 25% of VTA dopamine neurons were inhibited by VP stimulation, suggesting that the  
243 majority of spontaneously active dopamine neurons examined under control conditions are not directly  
244 innervated by the VP. This further suggests that a subset of dopamine neurons (~25%) receive input from the  
245 VP that is not tonically active and may be recruited to decrease dopamine neuron population activity. It is  
246 important to note that other parameters of the dopamine neuron recorded such as firing rate and burst firing did  
247 not correlate with response to VP stimulation, suggesting that VP activity regulates population activity  
248 specifically. Indeed, previous studies have demonstrated that chronic mild stress produces significant decreases  
249 in dopamine neuron population activity that are dependent on an increased VP drive from the basolateral  
250 amygdala that may be associated with symptoms of major depressive disorder(Chang & Grace, 2013a). It should  
251 be noted that previous studies have not reported decreased dopamine neuron population activity following  
252 activation of the VP(Floresco et al., 2003); however, these studies used bicuculline, a GABA<sub>A</sub> receptor  
253 antagonist, suggesting that the VP inputs to the VTA may not be tonically inhibited but can be activated by  
254 glutamatergic afferents to modulate dopamine neuron activity. Furthermore, a small population of VTA dopamine  
255 neurons (~10%) were activated by VP stimulation. Several reasons could underlie this observation. The first is  
256 that, the VP innervates a number of non-dopaminergic neurons in the VTA(Faget et al., 2016). VP inhibition of  
257 VTA GABA interneurons would, therefore, result in the activation of a small proportion of dopamine neurons.  
258 The other potential rationale is that glutamate may be co-released by a subset of VP neurons, as previous studies  
259 have reported that ~25% of VP projections to the VTA are positive for VGlut2, a vesicular glutamate  
260 transporter(Palmer et al., 2024). Our anatomical data indicate that roughly half of VP-targeted VTA neurons are  
261 not TH-positive, consistent with projections to local GABAergic and glutamatergic neurons. These non-  
262 dopaminergic populations may contribute to VP influence over VTA output by providing feedforward inhibition or

excitation of dopamine neurons, or by engaging downstream targets directly. Although not examined functionally here, their potential roles warrant further investigation.

The current literature posits that a tonic drive from the VP results in the inhibition of a significant population of VTA dopamine neurons under control conditions (Aguilar, 2014; Floresco et al., 2003; Palmer et al., 2024; Root et al., 2015). Therefore, it is impractical to examine whether these dopamine neurons are inhibited by VP stimulation if they are not spontaneously active. To address this caveat, we activated the vHipp, which is known to reduce VP drive to the VTA and increase the number of spontaneously active dopamine neurons (Perez & Lodge, 2018). It is important to note that our observed increase in dopamine neuron population activity was slightly lower than what has been reported in previous studies (Lodge & Grace, 2006), and this may raise the question of whether all VP-inhibited dopamine neurons were fully disinhibited. It is possible that repeated VP stimulation may lead to slight suppression in the number of spontaneously active dopamine neurons, suggesting that our reported number of inhibited neurons may be an underestimation of the actual number. Nevertheless, we found that the number of dopamine neurons inhibited by VP stimulation drastically increased. These findings suggest that a significant proportion of VTA dopamine neurons (~50%) receive input from the VP and that under control conditions, these inputs provide a tonic inhibition over a subpopulation of VTA dopamine neurons.

To confirm our physiological findings, we used a monosynaptic tracer to anatomically map the projections from the VP to the VTA. We found that about half of the dopamine neurons in the VTA received monosynaptic innervation from VP, consistent with data from our electrophysiology experiments. Interestingly, a significant number of non-dopamine cells were also innervated by the VP. The VTA is comprised of ~60% dopamine neurons, ~35% GABA neurons, and only ~5% glutamate neurons; thus, these other cells innervated by the VP are likely predominantly GABA-ergic (Nair-Roberts et al., 2008). These non-dopaminergic populations may contribute to VP influence over VTA output by providing feedforward inhibition or excitation of dopamine neurons, or by engaging downstream targets directly. Although not examined functionally here, this may correlate with our electrophysiological findings that a small proportion of VTA dopamine neurons are excited by VP stimulation, as inhibition of GABAergic interneurons may lead to excitation of dopamine neurons. These potential roles warrant further investigation. While the VP regulation of dopamine neurons in the VTA has been implicated in a

289 variety of pathological conditions(Soares-Cunha & Heinsbroek, 2023; Sonnenschein et al., 2020), the  
290 consequence of VP regulation of GABAergic cells is less well studied and requires further elucidation.

291 One caveat of our studies are the limitations of H129-derived anterograde tracers. H129-dTK vectors may fail to  
292 yield high labeling intensity due to limited fluorescent protein level(Zeng et al., 2017); thus, we amplified the  
293 signal using immunohistochemistry. However, the occurrence of incomplete labeling may have led  
294 underestimation of total number of VP-innervated neurons in VTA. Additionally, viral tropism could introduce cell-  
295 type biases that favor transfection of certain neuronal subpopulations. Finally, despite H129 primarily labeling in  
296 an anterograde manner, H129 is occasionally transported retrogradely from terminals in the injected regions. As  
297 a consequence, we cannot fully rule out the possibility that some labelled cells are VP-projecting neurons from  
298 VTA. These caveats suggest that our estimate of ~50% VP innervation should be interpreted as an  
299 approximation rather than an absolute measure of connectivity.

300 Previous studies have identified subregion-specific projection patterns from the VP to the VTA(Root et al., 2015;  
301 Soares-Cunha & Heinsbroek, 2023; Zahm et al., 2011). The VP is divided into distinct subregions based on  
302 functional anatomy and projection targets, with the ventromedial subregion exhibiting the strongest projections  
303 to the VTA(Root et al., 2015; Soares-Cunha & Heinsbroek, 2023). Based on this evidence, our coordinates for  
304 VP were selected to focus on this ventromedial region. To investigate whether the VP projections to the VTA  
305 resided in a specific subregion, we evaluated the distribution of dopamine neurons innervated by VP across the  
306 medial/lateral and anterior/posterior axes of the VTA. Comparisons of colocalized cells along these axes of the  
307 VTA revealed no significant differences, suggesting that VP afferents are evenly distributed throughout the VTA.  
308 Consistent with this finding, anterograde tracing with Phaseolus vulgaris-leucoagglutinin injected into the VP  
309 resulted in robust labeling of the VTA without evidence of spatially distinct projection patterns(Zahm et al., 2011).  
310 These findings suggest that the VP-VTA pathway operates in a spatially heterogeneous manner, allowing the  
311 VP to exert widespread influence over dopamine neuron activity across the VTA. Another important  
312 consideration is the cellular heterogeneity within VP itself. The VP contains multiple projection neuron classes,  
313 including purely GABAergic neurons, purely glutamatergic neurons, and a population that co-releases GABA  
314 and glutamate(Root et al., 2018 Jun 19). This observation indicates that at least part of the VP input to DA  
315 neurons may be excitatory or modulatory rather than purely inhibitory. Such heterogeneity likely contributes to

316 the diverse functional outcomes observed in our recordings, where VP stimulation produces inhibition in some  
317 dopamine units but had little effect, or even promoted firing, in others. Moreover, as discussed above, the  
318 observation that the VP projects to non-dopaminergic neurons further confounds the interpretation where multi-  
319 synaptic increases and decreases in dopamine neuron firing may be observed. Co-release adds an additional  
320 layer of complexity, as glutamate transmission can depolarize dopamine neurons, making them more susceptible  
321 to shunting inhibition from concurrent GABA<sub>A</sub> receptor activation, or alternatively drive rebound firing following  
322 GABAergic inhibition. Integrating these findings with the known diversity of VP outputs supports a model in which  
323 VP exerts a nuanced, projection- and state-dependent control over dopamine neuron population activity rather  
324 than acting as a purely inhibitory gate.

325 The apparent discrepancy between the proportion of dopamine neurons anatomically innervated by VP (~50%)  
326 and those functionally inhibited under baseline conditions (~25%) may partly reflect the tonic nature of VP output.  
327 VP neurons are known to fire tonically at rest(Clark, 2020) and provide a persistent GABAergic tone to  
328 VTA(Floresco et al., 2001; Floresco et al., 2003; Sesack & Grace, 2009). This tonic input likely holds a substantial  
329 fraction of dopamine neurons below firing threshold, effectively rendering them 'silent' in our population sample.  
330 Consequently, these neurons cannot be detected as inhibited by additional VP stimulation because they are  
331 already suppressed. vHipp activation, by engaging the NAc→VP pathway, reduces VP activity and disinhibits  
332 these quiescent DA neurons, increasing population activity. Once these neurons enter the spiking pool, VP  
333 stimulation can reveal their latent sensitivity, resulting in the larger proportion (>50%) of inhibited DA neurons  
334 observed after vHipp drive which is consistent with the anatomical data.

335 Beyond tonic inhibition and state-dependent sampling, other mechanisms may also contribute to this apparent  
336 disparity in control animals. VP terminals likely exhibit variability in synaptic strength and release probability,  
337 such that weaker inputs may only exert detectable effects when dopamine neurons are depolarized (although  
338 we did not see a correlation between baseline firing frequency and the effect of VP stimulation). Some VP  
339 terminals could represent functionally quiescent synapses lacking postsynaptic GABA<sub>A</sub> receptors or expressing  
340 primarily GABA<sub>B</sub> receptors that produce slower, subthreshold inhibition (see if there are references to support  
341 this). Postsynaptic heterogeneity is also well described among dopamine neuron subtypes, with differences in  
342 chloride driving force, GABA receptor expression, and intrinsic excitability that may shape their responsiveness

343 to VP input(Ford et al., 2006 Mar 8; Lammel et al., 2008). Finally, VP projections to VTA are phenotypically  
344 diverse, with both GABAergic and glutamatergic terminals (and possible co-release), and target both VTA GABA  
345 and dopamine neurons(Soares-Cunha & Heinsbroek, 2023). Together, these factors provide a mechanistic  
346 framework that reconciles our anatomical tracing data with the observed functional inhibition and underscores  
347 the dynamic, state-dependent influence of VP on dopamine population activity.

348 Dopamine neuron population activity has gained increasing attention over the last 20 years, as it is thought to  
349 provide a gain-of-function to the dopamine system, allowing for modulation of the number of spontaneously  
350 active dopamine neurons available to respond to behaviorally relevant stimuli(Grace, 2016). This form of  
351 regulation is essential for assigning salience to environmental cues and ensuring appropriate behavioral  
352 responses(Berridge & Robinson, 1998). Disruptions in this process have been implicated in a range of  
353 neuropsychiatric disorders. For example, decreases in dopamine neuron population activity following chronic  
354 stress have been associated with the pathophysiology of depression, leading to blunted dopaminergic responses  
355 and despair-like phenotypes dependent on actions through the basolateral amygdala(Chang & Grace, 2013a,  
356 2013b). Conversely, rodent models used to study schizophrenia, such as the methylazoxymethanol acetate  
357 (MAM) model, show a significant *increase* in dopamine neuron population activity, via hippocampal hyperactivity,  
358 which contributes to aberrant salience attribution and the emergence of positive symptoms(Lodge, 2013; Lodge  
359 & Grace, 2007, 2008b). Moreover, acute stressors such as foot shock have also been shown to increase  
360 dopamine neuron population activity, indicating that stress can profoundly modulate dopaminergic tone  
361 chronically and acutely(Elam et al., 2021; McCoy et al., 2022). Similar enhancements in dopamine system  
362 function have been observed in the context of substance abuse, where repeated administration of  
363 psychostimulant drugs like amphetamine increase dopamine neuron population activity leading to behavioral  
364 sensitization (Lodge & Grace, 2008a). Taken together, understanding of the afferent regulation of dopamine  
365 neuron population activity is of central importance. Under physiological conditions, such input may help fine-tune  
366 salience or reward processing by calibrating the dopaminergic gain in response to internal states or external  
367 cues. However, in pathological states, alterations in VP function could lead to maladaptive dopamine system  
368 output, contributing to the behavioral and cognitive impairments observed across a range of psychiatric  
369 disorders. Thus, delineating the various circuitries that regulate dopamine neuron population activity, particularly

370 under conditions that model psychiatric illness, provides a valuable framework for identifying potential therapeutic  
371 targets aimed at restoring dopamine system function.

372 Here we provide important information examining the mechanisms underlying this critical regulator of dopamine  
373 system function that is essential for our understanding of both normal salience function as well as a number of  
374 psychiatric disorders. Specifically, the observation that the VP does not innervate all dopamine neurons in the  
375 VTA suggests that innervated neurons may belong to distinct groups, likely characterized by specific molecular  
376 phenotypes and potentially projection patterns. Indeed, dopamine neurons project to a wide variety of cortical  
377 and subcortical regions including medial prefrontal cortex, ventral striatum, and amygdala (Haber et al., 1985).  
378 Studies by Floresco and Grace have demonstrated increases in tonic dopamine efflux in the NAc following VP  
379 inactivation suggesting that the VTA-NAc neurons may be preferentially innervated by the VP (Floresco et al.,  
380 2003); however, this requires further elucidation. Future studies will focus on classifying the precise phenotypes  
381 of both dopamine and non-dopamine neurons in the VTA that receive innervation from the VP as well as their  
382 specific projection targets. Taken together, these findings have important implications for better understanding  
383 the neuropathology underlying various psychiatric disorders, informing the development of targeted therapeutic  
384 interventions.

385 **Data Availability Statement:** All data supporting this article will be shared upon reasonable request to the  
386 corresponding author.

eNeuro Accepted Manuscript

## REFERENCES:

- Abi-Dargham, A. (2004). Do we still believe in the dopamine hypothesis? New data bring new evidence. *Int J Neuropsychopharmacol*, 7 Suppl 1, S1–5.
- Abi-Dargham, A., Gil, R., Krystal, J., Baldwin, R. M., Seibyl, J. P., Bowers, M., van Dyck, C. H., Charney, D. S., Innis, R. B., & Laruelle, M. (1998). Increased striatal dopamine transmission in schizophrenia: confirmation in a second cohort. *Am J Psychiatry*, 155(6), 761–767.
- Aguilar, D. D., Chen, L. & Lodge, D. J. (2014). Increasing Endocannabinoid Levels in the Ventral Pallidum Restores Aberrant Dopamine Neuron Activity in the Subchronic PCP Rodent Model of Schizophrenia. *Int J Neuropsychopharmacol*.
- Ashok, A. H., Marques, T. R., Jauhar, S., Nour, M. M., Goodwin, G. M., Young, A. H., & Howes, O. D. (2017). The dopamine hypothesis of bipolar affective disorder: the state of the art and implications for treatment. *Molecular Psychiatry*, 22(5). <https://doi.org/10.1038/mp.2017.16>
- Baik, J.-H., & Baik, J.-H. (2020). Stress and the dopaminergic reward system. *Experimental & Molecular Medicine* 2020 52:12, 52(12). <https://doi.org/10.1038/s12276-020-00532-4>
- Belujon, P., & Grace, A. A. (2014). Restoring mood balance in depression: ketamine reverses deficit in dopamine-dependent synaptic plasticity. *Biol Psychiatry*, 76(12), 927–936. <https://doi.org/10.1016/j.biopsych.2014.04.014>
- Berridge, K. C., & Robinson, T. E. (1998). What is the role of dopamine in reward: hedonic impact, reward learning, or incentive salience? *Brain Research Reviews*, 28(3). [https://doi.org/10.1016/S0165-0173\(98\)00019-8](https://doi.org/10.1016/S0165-0173(98)00019-8)
- Chang, C.-h., & Grace, A. A. (2013a). Amygdala-ventral pallidum pathway decreases dopamine activity following chronic mild stress in rats. *Biological psychiatry*, 76(3). <https://doi.org/10.1016/j.biopsych.2013.09.020>
- Chang, C.-h., & Grace, A. A. (2013b). Amygdala  $\beta$ -Noradrenergic Receptors Modulate Delayed Downregulation of Dopamine Activity following Restraint. *The Journal of Neuroscience*, 33(4). <https://doi.org/10.1523/JNEUROSCI.2420-12.2013>
- Clark, M. (2020). Effects of Electrical Stimulation of NAc Afferents on VP Neurons' Tonic Firing. *Frontiers in Cellular Neuroscience*, 14. <https://doi.org/10.3389/fncel.2020.599920>
- Compean, E., & Hamner, M. (2019). Posttraumatic stress disorder with secondary psychotic features (PTSD-SP): Diagnostic and treatment challenges. *Prog Neuropsychopharmacol Biol Psychiatry*, 88, 265–275. <https://doi.org/10.1016/j.pnpbp.2018.08.001>
- Egerton, A., Chaddock, C. A., Winton-Brown, T. T., Bloomfield, M. A. P., Bhattacharyya, S., Allen, P., McGuire, P. K., & Howes, O. D. (2013). Presynaptic striatal dopamine dysfunction in people at ultra-high risk for psychosis: Findings in a second cohort. *Biological psychiatry*, 74(2), 106–112.
- Elam, H. B., McCoy, A. M., Boley, A. M., Yang, O. J., Belle, N. I., & Lodge, D. J. (2025). Inhibition of Hippocampal or Thalamic Inputs to the Nucleus Accumbens Reverses Stress-induced Alterations in Dopamine System Function. *International Journal of Neuropsychopharmacology*. <https://doi.org/10.1093/ijnp/pyaf034>
- Elam, H. B., Perez, S. M., Donegan, J. J., & Lodge, D. J. (2021). Orexin receptor antagonists reverse aberrant dopamine neuron activity and related behaviors in a rodent model of stress-induced psychosis. *Transl Psychiatry*, 11(1), 114. <https://doi.org/10.1038/s41398-021-01235-8>
- Faget, L., Osakada, F., Duan, J., Ressler, R., Johnson, A. B., Proudfoot, J. A., Yoo, J. H., Callaway, E. M., & Hnasko, T. S. (2016). Afferent inputs to neurotransmitter-defined cell types in the ventral tegmental area. *Cell reports*, 15(12). <https://doi.org/10.1016/j.celrep.2016.05.057>
- Finlay, J. M., & Zigmond, M. J. (1997). The effects of stress on central dopaminergic neurons: possible clinical implications. *Neurochem Res*, 22(11), 1387–1394. <https://doi.org/10.1023/a:1022075324164>
- Floresco, S. B., Todd, C. L., & Grace, A. A. (2001). Glutamatergic afferents from the hippocampus to the nucleus accumbens regulate activity of ventral tegmental area dopamine neurons. *J Neurosci*, 21(13), 4915–4922.
- Floresco, S. B., West, A. R., Ash, B., Moore, H., & Grace, A. A. (2003). Afferent modulation of dopamine neuron firing differentially regulates tonic and phasic dopamine transmission. *Nat Neurosci*, 6(9), 968–973.

- 441 Ford, C. P., Mark, G. P., & Williams, J. T. (2006 Mar 8). Properties and Opioid Inhibition of Mesolimbic  
 442 Dopamine Neurons Vary according to Target Location. *The Journal of Neuroscience*, 26(10).  
 443 <https://doi.org/10.1523/JNEUROSCI.4331-05.2006>
- 444 Grace, A. A. (1995). The tonic/phasic model of dopamine system regulation: its relevance for understanding  
 445 how stimulant abuse can alter basal ganglia function. *Drug Alcohol Depend*, 37(2), 111–129.
- 446 Grace, A. A. (2000). The tonic/phasic model of dopamine system regulation and its implications for  
 447 understanding alcohol and psychostimulant craving. *Addiction*, 95 Suppl 2, S119–128.
- 448 Grace, A. A. (2016). Dysregulation of the dopamine system in the pathophysiology of schizophrenia and  
 449 depression. *Nat Rev Neurosci*, 17(8), 524–532. <https://doi.org/10.1038/nrn.2016.57>
- 450 Grace, A. A., & Bunney, B. S. (1983a). Intracellular and extracellular electrophysiology of nigral dopaminergic  
 451 neurons--1. Identification and characterization. *Neuroscience*, 10(2), 301–315.
- 452 Grace, A. A., & Bunney, B. S. (1983b). Intracellular and extracellular electrophysiology of nigral dopaminergic  
 453 neurons--1. Identification and characterization - PubMed. *Neuroscience*, 10(2).  
 454 [https://doi.org/10.1016/0306-4522\(83\)90135-5](https://doi.org/10.1016/0306-4522(83)90135-5)
- 455 Grace, A. A., & Bunney, B. S. (1984a). The control of firing pattern in nigral dopamine neurons: burst firing. *J*  
 456 *Neurosci*, 4(11), 2877–2890.
- 457 Grace, A. A., & Bunney, B. S. (1984b). The control of firing pattern in nigral dopamine neurons: single spike  
 458 firing. *J Neurosci*, 4(11), 2866–2876.
- 459 Grace, A. A., & Bunney, B. S. (1985). Opposing effects of striatonigral feedback pathways on midbrain  
 460 dopamine cell activity. *Brain Res*, 333(2), 271–284.
- 461 Haber, S., Groenewegen, H., Grove, E., & Nauta, W. (1985). Efferent connections of the ventral pallidum:  
 462 evidence of a dual striato pallidofugal pathway - PubMed. *The Journal of comparative neurology*,  
 463 235(3). <https://doi.org/10.1002/cne.902350304>
- 464 Howes, O. D., Kambeitz, J., Kim, E., Stahl, D., Slifstein, M., Abi-Dargham, A., & Kapur, S. (2012). The nature  
 465 of dopamine dysfunction in schizophrenia and what this means for treatment: Meta-analysis of imaging  
 466 studies. *Archives of general psychiatry*, 69(8), 776–786.
- 467 Howes, O. D., Montgomery, A. J., Asselin, M. C., Murray, R. M., Valli, I., Tabraham, P., Bramon-Bosch, E.,  
 468 Valmaggia, L., Johns, L., Broome, M., McGuire, P. K., & Grasby, P. M. (2009). Elevated striatal  
 469 dopamine function linked to prodromal signs of schizophrenia. *Arch Gen Psychiatry*, 66(1), 13–20.  
 470 <https://doi.org/10.1001/archgenpsychiatry.2008.514>
- 471 Kapur, S. (2003). Psychosis as a state of aberrant salience: a framework linking biology, phenomenology, and  
 472 pharmacology in schizophrenia - PubMed. *The American journal of psychiatry*, 160(1).  
 473 <https://doi.org/10.1176/appi.ajp.160.1.13>
- 474 Klein, M., Battagello, D., Cardoso, A., Hauser, D., Bittencourt, J., & Correa, R. (2019). Dopamine: Functions,  
 475 Signaling, and Association with Neurological Diseases - PubMed. *Cellular and molecular neurobiology*,  
 476 39(1). <https://doi.org/10.1007/s10571-018-0632-3>
- 477 Lammel, S., Hetzel, A., Häackel, O., Jones, I., Liss, B., & Roeper, J. (2008). Unique Properties of  
 478 Mesoprefrontal Neurons within a Dual Mesocorticolimbic Dopamine System. *Neuron*, 57(5), 760–773.  
 479 <https://doi.org/http://dx.doi.org/10.1016/j.neuron.2008.01.022>
- 480 Laruelle, M., & Abi-Dargham, A. (1999). Dopamine as the wind of the psychotic fire: new evidence from brain  
 481 imaging studies. *J Psychopharmacol*, 13(4), 358–371.
- 482 Li, Y.-D., Luo, Y.-J., Xu, W., Ge, J., Cherasse, Y., Wang, Y.-Q., Lazarus, M., Qu, W.-M., Huang, Z.-L., Li, Y.-D.,  
 483 Luo, Y.-J., Xu, W., Ge, J., Cherasse, Y., Wang, Y.-Q., Lazarus, M., Qu, W.-M., & Huang, Z.-L. (2020).  
 484 Ventral pallidal GABAergic neurons control wakefulness associated with motivation through the ventral  
 485 tegmental pathway. *Molecular Psychiatry* 2020 26:7, 26(7). <https://doi.org/10.1038/s41380-020-00906-0>
- 486 0
- 487 Lodge, D. J. (2011). The medial prefrontal and orbitofrontal cortices differentially regulate dopamine system  
 488 function. *Neuropsychopharmacology*, 36(6), 1227–1236. <https://doi.org/10.1038/npp.2011.7>
- 489 Lodge, D. J. (2013). The MAM rodent model of schizophrenia. *Curr Protoc Neurosci*, Chapter 9, Unit9.43.  
 490 <https://doi.org/10.1002/0471142301.ns0943s63>
- 491 Lodge, D. J., & Grace, A. A. (2006). The hippocampus modulates dopamine neuron responsivity by regulating  
 492 the intensity of phasic neuron activation. *Neuropsychopharmacology*, 31(7), 1356–1361.

- 493 Lodge, D. J., & Grace, A. A. (2007). Aberrant hippocampal activity underlies the dopamine dysregulation in an  
 494 animal model of schizophrenia. *J Neurosci*, *27*(42), 11424–11430.  
 495 <https://doi.org/10.1523/JNEUROSCI.2847-07.2007>
- 496 Lodge, D. J., & Grace, A. A. (2008a). Amphetamine activation of hippocampal drive of mesolimbic dopamine  
 497 neurons: a mechanism of behavioral sensitization. *J Neurosci*, *28*(31), 7876–7882.
- 498 Lodge, D. J., & Grace, A. A. (2008b). Hippocampal dysfunction and disruption of dopamine system regulation  
 499 in an animal model of schizophrenia. *Neurotox Res*, *14*(2-3), 97–104.
- 500 Lodge, D. J., & Grace, A. A. (2009). Gestational methylazoxymethanol acetate administration: A  
 501 developmental disruption model of schizophrenia. *Behav Brain Res*, *7*(204(2)), 306–312.
- 502 Lunde, A., Glover, J. C., Lunde, A., & Glover, J. C. (2020–11–04). A versatile toolbox for semi-automatic cell-  
 503 by-cell object-based colocalization analysis. *Scientific Reports 2020 10:1*, 10(1).  
 504 <https://doi.org/10.1038/s41598-020-75835-7>
- 505 Mahler, S. V., Vazey, E. M., Beckley, J. T., Keistler, C. R., McGlinchey, E. M., Kaufling, J., Wilson, S. P.,  
 506 Deisseroth, K., Woodward, J. J., Aston-Jones, G., Mahler, S. V., Vazey, E. M., Beckley, J. T., Keistler,  
 507 C. R., McGlinchey, E. M., Kaufling, J., Wilson, S. P., Deisseroth, K., Woodward, J. J., & Aston-Jones,  
 508 G. (2014). Designer receptors show role for ventral pallidum input to ventral tegmental area in cocaine  
 509 seeking. *Nature Neuroscience 2014 17:4*, 17(4). <https://doi.org/10.1038/nn.3664>
- 510 McCoy, A. M., Prevot, T. D., Mian, M. Y., Cook, J. M., Frazer, A., Sibille, E. L., Carreno, F. R., & Lodge, D. J.  
 511 (2022). Positive Allosteric Modulation of alpha5-GABAA Receptors Reverses Stress-Induced  
 512 Alterations in Dopamine System Function and Prepulse Inhibition of Startle. *Int J*  
 513 *Neuropsychopharmacol*, *25*(8), 688–698. <https://doi.org/10.1093/ijnp/pyac035>
- 514 Nair-Roberts, R., Chatelain-Badie, S., Benson, E., White-Cooper, H., Bolam, J., & Ungless, M. (2008).  
 515 Stereological estimates of dopaminergic, GABAergic and glutamatergic neurons in the ventral  
 516 tegmental area, substantia nigra and retrorubral field in the rat - PubMed. *Neuroscience*, *152*(4).  
 517 <https://doi.org/10.1016/j.neuroscience.2008.01.046>
- 518 Palaniyappan, L., & Liddle, P. F. (2012). Does the salience network play a cardinal role in psychosis? An  
 519 emerging hypothesis of insular dysfunction. *Journal of Psychiatry & Neuroscience : JPN*, *37*(1).  
 520 <https://doi.org/10.1503/jpn.100176>
- 521 Palmer, D., Cayton, C. A., Scott, A., Lin, I., Newell, B., Paulson, A., Weberg, M., & Richard, J. M. (2024).  
 522 Ventral pallidum neurons projecting to the ventral tegmental area reinforce but do not invigorate  
 523 reward-seeking behavior. *Cell reports*, *43*(1). <https://doi.org/10.1016/j.celrep.2023.113669>
- 524 Paxinos, G., Watson, C. . (1998). *The rat brain in stereotaxic coordinates*. Academic Press.
- 525 Perez, S. M., Elam, H. B., & Lodge, D. J. (2022). Increased Presynaptic Dopamine Synthesis Capacity Is  
 526 Associated With Aberrant Dopamine Neuron Activity in the Methylazoxymethanol Acetate Rodent  
 527 Model Used to Study Schizophrenia-Related Pathologies. *Schizophrenia bulletin open*, *3*(1).  
 528 <https://doi.org/10.1093/schizbullopen/sgac067>
- 529 Perez, S. M., & Lodge, D. J. (2018). Convergent Inputs from the Hippocampus and Thalamus to the Nucleus  
 530 Accumbens Regulate Dopamine Neuron Activity. *J Neurosci*, *38*(50), 10607–10618.  
 531 <https://doi.org/10.1523/JNEUROSCI.2629-16.2018>
- 532 Root, D. H., Melendez, R. I., Zaborszky, L., & Napier, T. C. (2015). The ventral pallidum: Subregion-specific  
 533 functional anatomy and roles in motivated behaviors. *Progress in neurobiology*, *130*.  
 534 <https://doi.org/10.1016/j.pneurobio.2015.03.005>
- 535 Root, D. H., Zhang, S., Barker, D. J., Miranda-Barrientos, J., Liu, B., Wang, H.-L., & Morales, M. (2018 Jun 19).  
 536 Selective Brain Distribution and Distinctive Synaptic Architecture of Dual Glutamatergic-GABAergic  
 537 Neurons. *Cell reports*, *23*(12). <https://doi.org/10.1016/j.celrep.2018.05.063>
- 538 Sesack, S. R., & Grace, A. A. (2009). Cortico-Basal Ganglia Reward Network: Microcircuitry.  
 539 *Neuropsychopharmacology*, *35*(1). <https://doi.org/10.1038/npp.2009.93>
- 540 Soares-Cunha, C., & Heinsbroek, J. A. (2023). Frontiers | Ventral pallidal regulation of motivated behaviors  
 541 and reinforcement. *Frontiers in Neural Circuits*, *17*. <https://doi.org/10.3389/fncir.2023.1086053>
- 542 Sonnenschein, S. F., Gomes, F. V., & Grace, A. A. (2020). Dysregulation of Midbrain Dopamine System and  
 543 the Pathophysiology of Schizophrenia. *Frontiers in Psychiatry*, *11*.  
 544 <https://doi.org/10.3389/fpsy.2020.00613>
- 545 Ungless, M. A., & Grace, A. A. (2012). Are you or aren't you? Challenges associated with physiologically  
 546 identifying dopamine neurons. *Trends in Neurosciences*, *35*(7), 422–430.

- 547 Volkow, N. D., Fowler, J. S., Wang, G. J., & Swanson, J. M. (2004). Dopamine in drug abuse and addiction:  
548 results from imaging studies and treatment implications. *Mol Psychiatry*, 9(6), 557–569.  
549 <https://doi.org/10.1038/sj.mp.4001507>
- 550 Watabe-Uchida, M., Zhu, L., Ogawa, S., Vamanrao, A., & Uchida, N. (2012). Whole-brain mapping of direct  
551 inputs to midbrain dopamine neurons - PubMed. *Neuron*, 74(5).  
552 <https://doi.org/10.1016/j.neuron.2012.03.017>
- 553 Zahm, D. S., Cheng, A. Y., Lee, T. J., Ghobadi, C. W., Schwartz, Z. M., Geisler, S., Parsely, K. P., Gruber, C.,  
554 & Veh, R. W. (2011). Inputs to the Midbrain Dopaminergic Complex in the Rat with Emphasis on  
555 Extended Amygdala-recipient Sectors. *The Journal of comparative neurology*, 519(16).  
556 <https://doi.org/10.1002/cne.22670>
- 557 Zeng, W.-B., Jiang, H.-F., Gang, Y.-D., Song, Y.-G., Shen, Z.-Z., Yang, H., Dong, X., Tian, Y.-L., Ni, R.-J., Liu,  
558 Y., Tang, N., Li, X., Jiang, X., Gao, D., Androulakis, M., He, X.-B., Xia, H.-M., Ming, Y.-Z., Lu, Y.,...Luo,  
559 M.-H. (2017). Anterograde monosynaptic transneuronal tracers derived from herpes simplex virus 1  
560 strain H129. *Molecular Neurodegeneration* 2017 12:1, 12(1). [https://doi.org/10.1186/s13024-017-0179-](https://doi.org/10.1186/s13024-017-0179-7)  
561 [7](https://doi.org/10.1186/s13024-017-0179-7)

## FIGURE LEGENDS

**Table 1:** Statistical table indicating data structure and confidence intervals for all statistical analysis.

**Figure 1:** Schematic depicting afferent inputs to VP that modulate VTA dopamine neuron population activity and the role of these inputs in various pathological states. Ventral hippocampus (vHipp); paraventricular nucleus of the thalamus (PVT); nucleus accumbens (NAc); basolateral amygdala (BLA); ventral pallidum (VP); ventral tegmental area (VTA); major depressive disorder (MDD).

**Figure 2:** *The proportion of VTA dopamine neurons inhibited by VP stimulation increases after vHipp activation.*

**(A)** The proportion of VTA dopamine neurons unaffected, activated, or inhibited by VP stimulation after delivery of vehicle or NMDA into the vHipp. **(B)** The number of spontaneously active VTA dopamine neurons (population activity) after delivery of vehicle or NMDA into the vHipp. **(C)** Percent of action potentials firing in bursts **(D)** Firing frequency of recorded dopamine neurons at baseline and during VP stimulation. **(E-F)** Average firing frequency **(E)** or percent action potentials firing in bursts **(F)** of dopamine neurons unaffected, excited, or inhibited by VP stimulation. **(G-H)** Representative brain slices of **(G)** VP (gray square) with stimulating electrode placement (arrow), **(H)** vHipp (open square) with cannula placement (open arrow), and VTA (gray square) with recording electrode placement (black arrow). **(I)** Representative peri-stimulus time histograms for dopamine neurons unaffected, excited, or inhibited by VP stimulation. **(J)** Representative electrophysiology recording of dopamine neurons before and during VP stimulations (black bar) and action potential traces for dopamine neuron unaffected, excited, or inhibited by VP stimulation. \*\*\* $p < 0.001$

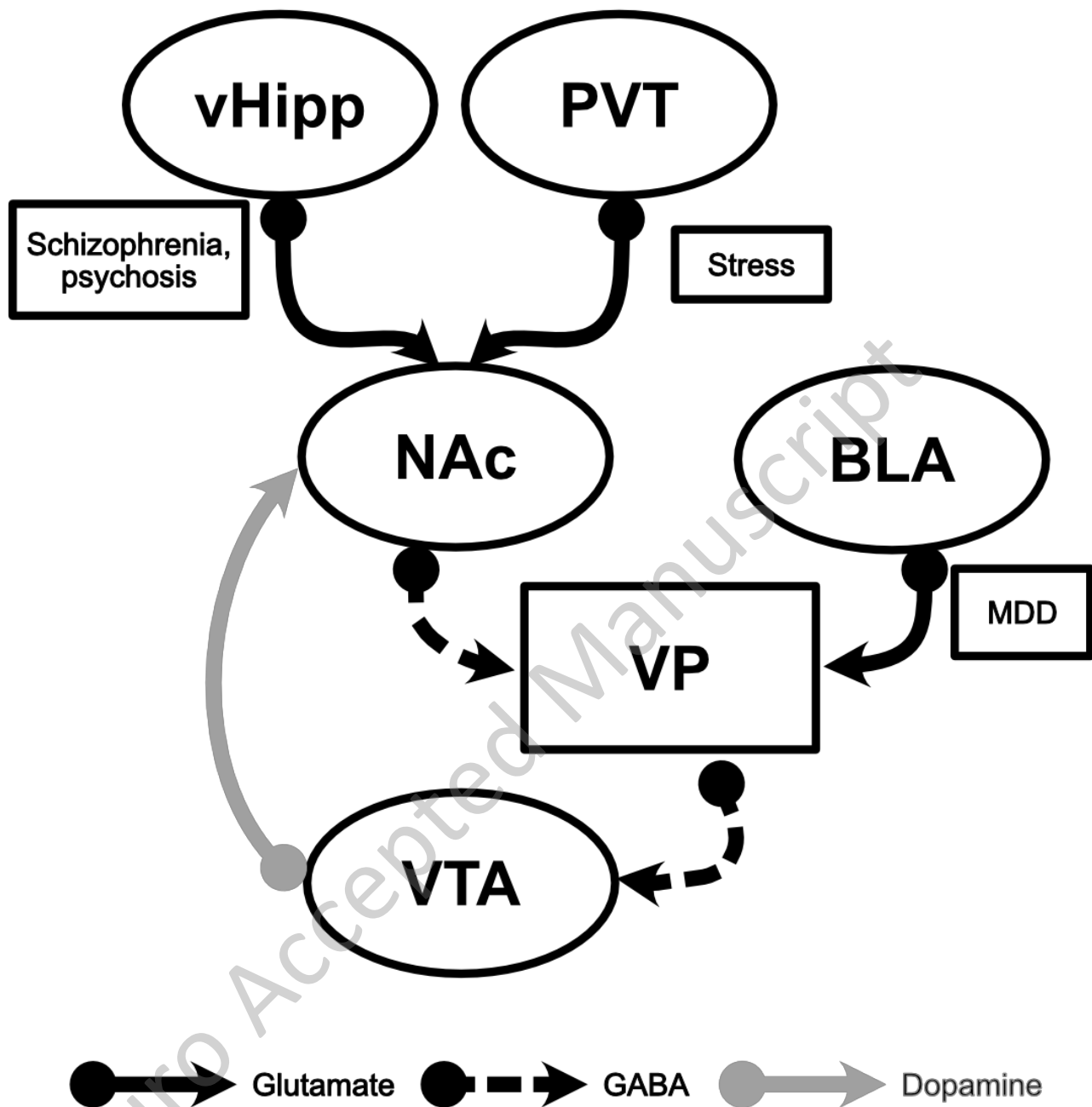
**Figure 3:** *The VP projects to a subset of VTA dopamine neurons.* **(A)** Schematic depicting monosynaptic labelling using H129 and helper virus and injection timeline. **(B)** Representative brain slice of VP with cannula placement (arrow). **(C)** Representative brain slice of mesencephalon containing VTA and tyrosine hydroxylase (TH) immuno-labelling (green). **(D)** Representative images of cells in VTA indicating colocalized cells (left, white circles), TH+ only cells (middle, green circles), and tdTomato (Td) + only cells (right, red circles). **(E)** Percent of TH+ cells colabelled with Td (left) and percent of Td+ cells colabelled with TH (right). **(F)** Number of colocalized cells along the medial(M)/lateral(L) axis. **(G)** Number of colocalized cells along the anterior (A)/posterior (P) axis.

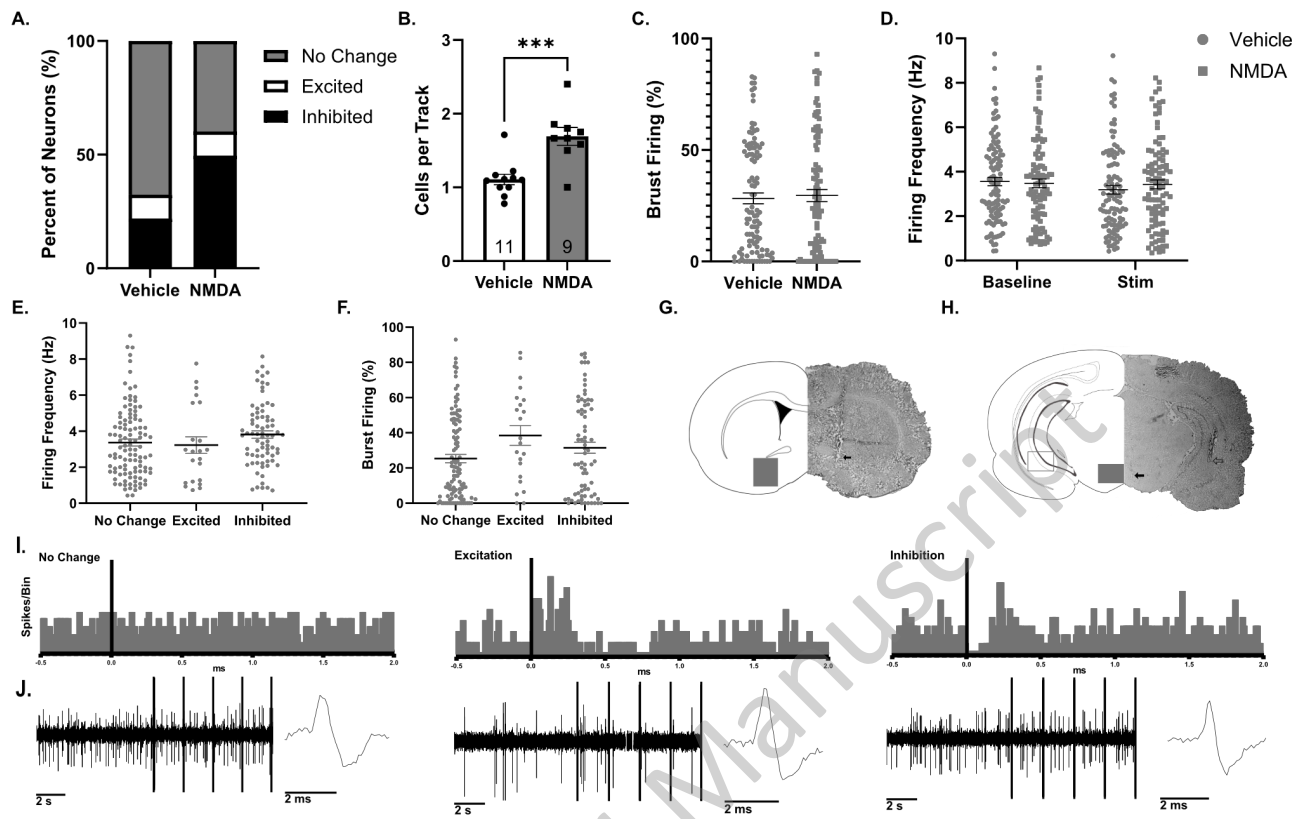
593 **Table 1:** Statistical Table

	<b>Figure</b>	<b>Data Structure</b>	<b>Type of Test</b>	<b>Power</b>
a	Figure 2A	Contingency table	Chi-Squared	N/A
b	Figure 2B	Normal distribution	<i>t</i> - test	95% CI [0.31,0.88]
c	Figure 2C	Not normally distributed	Mann-Whitney	95% CI [-5.0,6.2]
d	Figure 2D	Not normally distributed	Aligned Rank Transform (ART) ANOVA	95% CI Veh [188,221] NMDA [194,227] BL [198,231] Stim [184,217]
e	Figure 2E	Not normally distributed	Kruskal-Wallis	95% CI [2.98,3.72; 2.27,4.19; 3.41,4.23]
f	Figure 2F	Not normally distributed	Kruskal-Wallis	95% CI [20.92,30.05; 26.78,50.17; 25.25,37.75]
g	Figure 3E	Normal distribution	<i>t</i> - test	95% CI [-21.6 to 16.6]
h	Figure 3F	Normal distribution	One-way ANOVA	95% CI [20.64,50.27; 23.81,57.08; 19.66,64.76]
i	Figure 3G	Normal distribution	One-way ANOVA	95% CI [34.32,171.7; 105.4,210.6; 74.08,258.9; -0.4113,149.1]

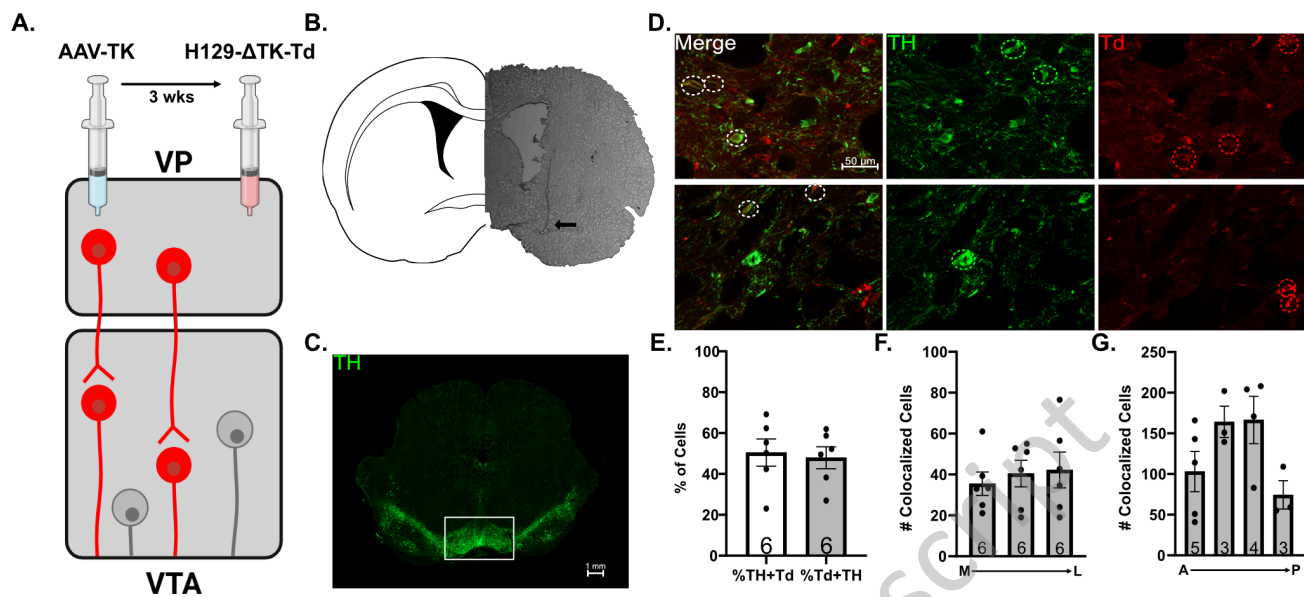
594

595





eNeuro Accepted Manuscript



eNeuro Accepted Manuscript